Comput Mech (2005)
DOI 10.1007/s00466-005-0719-9

ORIGINAL PAPER

J. T. Chen · C. S. Wu · K. H. Chen · Y. T. Lee

Degenerate scale for the analysis of circular thin plate using the boundary integral equation method and boundary element methods

Received: 20 October 2004 / Accepted: 13 May 2005 / Published online: 10 August 2005

Abstract In this paper, the degenerate scale for plate problem is studied. For the continuous model, we use the null-field integral equation, Fourier series and the series expansion in terms of degenerate kernel for fundamental solutions to examine the solvability of BIEM for circular thin plates. Any two of the four boundary integral equations in the plate formulation may be chosen. For the discrete model, the circulant is employed to determine the rank deficiency of the influence matrix. Both approaches, continuous and discrete models, lead to the same result of degenerate scale. We study the nonunique solution analytically for the circular plate and find degenerate scales. The similar properties of solvability condition between the membrane (Laplace) and plate (biharmonic) problems are also examined. The number of degenerate scales for the six boundary integral formulations is also determined.

Keywords Plate · Biharmonic problem · Degenerate scale · Boundary integral equation method · Boundary element method · Circulant

1 Introduction

During the recent decades, BEM has been recognized as an effective approach in numerical analysis over than the FDM and FEM for some specific problems. But, there are some pitfalls imbedded in the BEM, e.g., the degenerate scale [9, 12] and fictitious frequency [14] regarding to the solvability of formulations. Many treatments were employed to overcome the rank-deficiency problem e.g., rigid body motion method [13], SVD updating technique [13], Burton and Miller concept [10]. It is well known that the special geometry size may result in a nonunique solution for potential problems, and the size is coined degenerate scale. It means that the term "scale" stems from the fact that degenerate mechanism depends on the geometry size used when the BEM is implemented.

The degenerate scale problems (nonuniqueness) in BEM for potential problem [23] and plane elasticity [2, 17, 21, 22] have been done even for the plate problem (biharmonic equation) [18, 24] and numerical experiments have been performed [9]. Chen et al. [9, 12] have determined the degenerate scale for Laplace and Navier operators by using circulant and series expansion in terms of degenerate kernel for fundamental solutions [20]. For the degenerate scale of multiply-connected domain problems, Tomlinson et al. [30] and Mitra and Das [26] have solved for Laplace and biharmonic equations using BEM, respectively. In the recent work, Chen et al. [9] studied the degenerate scale for simply-connected and multiply-connected problems by using degenerate kernel and circulant in a discrete model for circular and annular cases. However, to the authors' best knowledge, the skill of degenerate kernel has not been employed to study the degenerate scale problem of plate. This paper employs the degenerate kernel as a mathematical tool to study the degenerate scale problem of plate.

From the mathematical point of view, we solve harmonic problems by means of Green's identity which leads to integral equations for the direct BEMs. This equation does not have a unique solution for certain boundary curves (Γ contour in [25]) and they are characterized by means of the logarithmic capacity [3,19] (or transfinite boundary, mapping radius, conformal radius). For a circle, the logarithmic capacity is equal to the radius. A rigorous study was proposed mathemati-

J. T. Chen (✉) · C. S. Wu · Y. T. Lee
Department of Harbor and River Engineering,
National Taiwan Ocean University,
Keelung, 20224 Taiwan
E-mail: jtchen@mail.ntou.edu.tw
Tel.: 886-2-2462-2192-ext. 6140 or 6177
Fax: 886-2-2463-2375

K. H. Chen
Department of Information Management,
Toko University, Chia-Yi, 613 Taiwan

cally by Chudinovich and Costanda [4–8, 17] and Christiansen [3] for the plate problem (biharmonic equation) on the occuring mechanism of the degenerate scale. Although mathematicians [3] also encountered the nonunique problem in BIEM, the addressed BIEs are not the same as those used by the BEM researchers. Numerical difficulties due to nonuniqueness of solutions have been overcome by employing the necessary and sufficient boundary integral equation (NSBIE) and boundary contour method [27, 29]. On the other hand, engineers always used the BEM program as a black box. Therefore, they may not understand the possible failure of the method and may take risk when a degenerate scale occurs. We will fill the gap between the mathematicians and engineers and demonstrate how the degenerate scale problem occurs.

In this paper, the biharmonic operator instead of the Laplacian or Navier operator is considered. The static plate problem is solved by using the BIEM and BEM in the continuous and discrete models, respectively. In the conventional BEM for the Laplace and the Navier problems, we have proved the existence of one (Laplace) and two (Navier) degenerate scales when the geometry is special. Theoretical results for the degenerate scale of biharmonic operator for rectangles and triangles have been done by Costabel and Dauge [19]. Numerical results using the symmetric Galerkin BEM for ellipse and multiply connected problems were also given by Vodička and Mantič [31]. The fact that the number of degenerate scales for the Navier equation can be one or two was also found [19]. Engineers always do not take notice of the number of degenerate scales for the biharmonic problem. Since any two boundary integral equations in the plate formulation (essential and natural sets) can be chosen, six (C_2^4) approaches can be considered. We may wonder how many degenerate scales may appear in the BIEM and BEM for plate problems. By using the six options, we have different degenerate scales for each choice. In the discrete model, the series expansion in terms of degenerate kernel for the fundamental solution and circulant are employed to study the rank-deficiency problem in the influence matrix. The occurring mechanism of degenerate scale for simply-connected plate problems in each formulation is studied analytically by using the continuous and discrete models. Besides, the similar properties of degenerate scale between the membrane (Laplace) and plate (biharmonic) problems are examined. The nontrivial modes, rigid body mode and spurious mode, for the Laplace and biharmonic problems are studied. Finally, the number of degenerate scales for each boundary integral formulation is determined.

2 Dual boundary integral equations for simply-connected biharmonic problems

Consider the Kirchhoff plate [1] under distributed load $w(x)$ as shown in Fig. 1, the governing equation is written as follows:

$$\nabla^4 u^*(x) = \frac{w(x)}{D}, \; x \in \Omega, \tag{1}$$

where $u^*(x)$ is the lateral displacement, D is the flexural rigidity of the plate expressed as $D = \frac{Eh^3}{12(1-\nu^2)}$ in terms of Young's modulus E, the Poisson ratio ν and the plate thickness h, and Ω is the domain of the thin plate. For the boundary conditions of the clamped case, simply-supported case and free case, we have

$$u^*(x) = 0, \theta^*(x) = 0, \quad x \in B, \tag{2}$$

$$u^*(x) = 0, m^*(x) = 0, \quad x \in B, \tag{3}$$

$$m^*(x) = 0, v^*(x) = 0, \quad x \in B \tag{4}$$

respectively, where B is the boundary, $\theta^*(x)$, $m^*(x)$ and $v^*(x)$ are the slope, normal moment and effective shear force, respectively. Since the governing equation contains the body force, the problem is reformulated to homogeneous PDE by using the splitting method as follows:

$$\nabla^4 u(x) = 0, \quad x \in \Omega, \tag{5}$$

and the essential boundary conditions are changed to

$$u(x) = \bar{u}(x), \frac{\partial u(x)}{\partial n} = \bar{\theta}(x), \quad x \in B. \tag{6}$$

The mixed-type boundary conditions are

$$u(x) = \bar{u}(x), m(x) = \bar{m}(x), \quad x \in B. \tag{7}$$

The natural boundary conditions are

$$m(x) = \bar{m}(x), v(x) = \bar{v}(x), \quad x \in B. \tag{8}$$

The operators of slope, normal moment and effective shear force are derived by

$$\theta(x) = \mathscr{K}_{\theta,x}(u(x)) = \frac{\partial u(x)}{\partial n_x}, \tag{9}$$

$$m(x) = \mathscr{K}_{m,x}(u(x)) = \nu \nabla_x^2 u(x) + (1-\nu)\frac{\partial^2 u(x)}{\partial n_x^2}, \tag{10}$$

$$v(x) = \mathscr{K}_{v,x}(u(x)) = \frac{\partial \nabla_x^2 u(x)}{\partial n_x} + (1-\nu)\frac{\partial}{\partial t_x}\left(\frac{\partial^2 u(x)}{\partial n_x \partial t_x}\right), \tag{11}$$

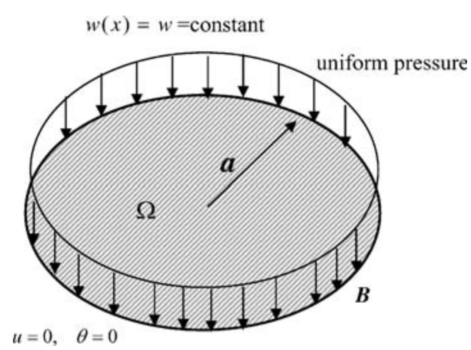

Fig. 1 The Kirchoff clamped plate under distributed load

where $\mathscr{K}_{\theta,x}(\cdot)$, $\mathscr{K}_{m,x}(\cdot)$ and $\mathscr{K}_{v,x}(\cdot)$ mean the operators with respect to x; n and t are the normal vector and tangential vector, respectively.

2.1 Mathematical formulation for biharmonic problems using the dual boundary integral equations

The integral equations for the domain point of biharmonic problems can be derived from the Rayleigh-Green identity as follows [16]:

$$8\pi u(x) = \int_B \{-U(s,x)v(s) + \Theta(s,x)m(s) - M(s,x)\theta(s) + V(s,x)u(s)\}\mathrm{d}B(s), \quad x \in \Omega, \quad (12)$$

$$8\pi\theta(x) = \int_B \{-U_\theta(s,x)v(s) + \Theta_\theta(s,x)m(s) - M_\theta(s,x)\theta(s) + V_\theta(s,x)u(s)\}\mathrm{d}B(s), \quad x \in \Omega, \quad (13)$$

$$8\pi m(x) = \int_B \{-U_m(s,x)v(s) + \Theta_m(s,x)m(s) - M_m(s,x)\theta(s) + V_m(s,x)u(s)\}\mathrm{d}B(s), \quad x \in \Omega, \quad (14)$$

$$8\pi v(x) = \int_B \{-U_v(s,x)v(s) + \Theta_v(s,x)m(s) - M_v(s,x)\theta(s) + V_v(s,x)u(s)\}\mathrm{d}B(s), \quad x \in \Omega, \quad (15)$$

where s and x are the source and field points, respectively, U, Θ, M, V, U_θ, Θ_θ, M_θ, V_θ, U_m, Θ_m, M_m, V_m, U_v, Θ_v, M_v and V_v are the kernel functions which are listed in Appendix A by using the series expansion in terms of degenerate kernel. The kernel function $U(s,x)$ is the fundamental solution which satisfies

$$\nabla_x^4 U(x,s) = 8\pi\delta(x-s), \quad (16)$$

where $\delta(x-s)$ is the Dirac-delta function. Then, we can obtain the fundamental solution as follows:

$$U(x,s) = r^2 lnr, \quad (17)$$

where r is the distance between x and s ($r = |x-s|$). We choose the null-field integral equations to study the degenerate scale problem analytically. Once the field point x locates outside the domain, the null-field BIEs in Eqs. (12)–(15) yield

$$0 = \int_B \{-U(s,x)v(s) + \Theta(s,x)m(s) - M(s,x)\theta(s) + V(s,x)u(s)\}\ \mathrm{d}B(s), \quad x \in \Omega^e, \quad (18)$$

$$0 = \int_B \{-U_\theta(s,x)v(s) + \Theta_\theta(s,x)m(s) - M_\theta(s,x)\theta(s) + V_\theta(s,x)u(s)\}\ \mathrm{d}B(s), \quad x \in \Omega^e, \quad (19)$$

$$0 = \int_B \{-U_m(s,x)v(s) + \Theta_m(s,x)m(s) - M_m(s,x)\theta(s) + V_m(s,x)u(s)\}\ \mathrm{d}B(s), \quad x \in \Omega^e, \quad (20)$$

$$0 = \int_B \{-U_v(s,x)v(s) + \Theta_v(s,x)m(s) - M_v(s,x)\theta(s) + V_v(s,x)u(s)\}\mathrm{d}B(s), \quad x \in \Omega^e, \quad (21)$$

where Ω^e is the complementary domain. By using the series expansion in terms of degenerate kernel, the BIE for the "boundary point" is derived easily through the null-field integral equation without the jump and free terms. When the boundary is uniformly discretized into $2N$ constant elements, the linear algebraic equations of Eqs. (18)–(21) by moving the field point x close to the boundary B^+ are obtained as follows:

$$[U_{ij}]\{v_j\} + [M_{ij}]\{\theta_j\} = [\Theta_{ij}]\{m_j\} + [V_{ij}]\{u_j\}, \quad (22)$$

$$[U_{ij}^\theta]\{v_j\} + [M_{ij}^\theta]\{\theta_j\} = [\Theta_{ij}^\theta]\{m_j\} + [V_{ij}^\theta]\{u_j\}, \quad (23)$$

$$[U_{ij}^m]\{v_j\} + [M_{ij}^m]\{\theta_j\} = [\Theta_{ij}^m]\{m_j\} + [V_{ij}^m]\{u_j\}, \quad (24)$$

$$[U_{ij}^v]\{v_j\} + [M_{ij}^v]\{\theta_j\} = [\Theta_{ij}^v]\{m_j\} + [V_{ij}^v]\{u_j\}, \quad (25)$$

where $[U_{ij}]$, $[\Theta_{ij}]$, $[M_{ij}]$, $[V_{ij}]$, $[U_{ij}^\theta]$, $[\Theta_{ij}^\theta]$, $[M_{ij}^\theta]$, $[V_{ij}^\theta]$, $[U_{ij}^m]$, $[\Theta_{ij}^m]$, $[M_{ij}^m]$, $[V_{ij}^m]$, $[U_{ij}^v]$, $[\Theta_{ij}^v]$, $[M_{ij}^v]$ and $[V_{ij}^v]$ are the sixteen influence matrices with a dimension $2N \times 2N$, $\{u_j\}$, $\{\theta_j\}$, $\{m_j\}$ and $\{v_j\}$ are the vectors of boundary data with a dimension $2N \times 1$. After substituting the boundary condition, we expand the sixteen kernel functions into series form in terms of degenerate kernels as shown in Appendix A and substitute them into boundary integral formulation in the continuous and discrete models. To derive the degenerate scale analytically, a circular plate is demonstrated.

2.2 Existence of the degenerate scale for a circular plate — continuous model (BIEM)

For the clamped, simply-supported and free circular plates, we demonstrate the existence of degenerate scale by employing the BIEs in the continuous model. Since any two BIEs in the plate formulation (essential and natural sets) are chosen, six (C_2^4) options are considered. Although a circular case lacks generality, it leads significant insight into the occurring mechanism of degenerate scale.

Case 1. Clamped plate

The moment and shear force, $m(s)$ and $v(s)$, are expanded into Fourier series as shown below:

$$m(s) = p_0^c + \sum_{n=1}^{\infty}(p_n^c \cos(n\theta) + q_n^c \sin(n\theta)), \quad s \in B, \quad (26)$$

$$v(s) = a_0^c + \sum_{n=1}^{\infty}(a_n^c \cos(n\theta) + b_n^c \sin(n\theta)), \quad s \in B, \tag{27}$$

where p_0^c, p_n^c, q_n^c, a_0^c, a_n^c and b_n^c are the undetermined Fourier coefficients for $m(s)$ and $v(s)$, θ is the angle on the circular boundary and the superscript c denotes the clamped case. By using the null-field integral equations of Eqs. (18) and (19), the clamped boundary conditions, $\overline{u}(s)$ and $\overline{\theta}(s)$, are substituted. By using the series expansion in terms of degenerate kernel and substituting the boundary densities in Eqs. (26) and (27) into the BIEs, we have

$$\begin{aligned} f_1^c(\phi) = &-\int_0^{2\pi} U(s,x)[a_0^c + \sum_{n=1}^{\infty}(a_n^c \cos(n\theta) \\ &+ b_n^c \sin(n\theta))]a\mathrm{d}\theta \\ &+ \int_0^{2\pi} \Theta(s,x)[p_0^c + \sum_{n=1}^{\infty}(p_n^c \cos(n\theta) \\ &+ q_n^c \sin(n\theta))]a\mathrm{d}\theta, \quad x \in B, \end{aligned} \tag{28}$$

$$\begin{aligned} f_2^c(\phi) = &-\int_0^{2\pi} U_\theta(s,x)[a_0^c + \sum_{n=1}^{\infty}(a_n^c \cos(n\theta) \\ &+ b_n^c \sin(n\theta))]a\mathrm{d}\theta \\ &+ \int_0^{2\pi} \Theta_\theta(s,x)[p_0^c + \sum_{n=1}^{\infty}(p_n^c \cos(n\theta) \\ &+ q_n^c \sin(n\theta))]a\mathrm{d}\theta, \quad x \in B, \end{aligned} \tag{29}$$

where $f_1^c(\phi)$ and $f_2^c(\phi)$ are the terms due to the specified boundary conditions. Moreover, f_1^c and f_2^c can be expressed in terms of Fourier series

$$f_1^c(\phi) = g_0^c + \sum_{n=1}^{\infty}[g_n^c \cos(n\phi) + h_n^c \sin(n\phi)] \tag{30}$$

$$f_2^c(\phi) = g_0^{*c} + \sum_{n=1}^{\infty}[g_n^{*c} \cos(n\phi) + h_n^{*c} \sin(n\phi)] \tag{31}$$

where the coefficients g_0^c, g_n^c, h_n^c, g_0^{*c}, g_n^{*c} and h_n^{*c} are all known. In this case, we have the $R = \rho = a$ for the direct BIEM and $\mathrm{d}B(s) = a\,\mathrm{d}\theta$ for the circular plate with radius a. By employing the orthogonality condition of the Fourier bases, we construct the relations of the Fourier coefficients among a_n^c, b_n^c, p_n^c and q_n^c. Combining the two integral equations in Eqs. (28) and (29) and comparing with the coefficients, we assemble them into the matrix forms as shown below:

$$[SM_m^e]_{2\times 2}\begin{Bmatrix} a_m^c \\ p_m^c \end{Bmatrix} = \begin{Bmatrix} g_m^c \\ g_m^{*c} \end{Bmatrix}, m = 0, 1, 2, 3, \ldots \tag{32}$$

$$[SM_m^o]_{2\times 2}\begin{Bmatrix} b_m^c \\ q_m^c \end{Bmatrix} = \begin{Bmatrix} g_m^{*c} \\ h_m^{*c} \end{Bmatrix}, m = 1, 2, 3, \ldots \tag{33}$$

where the coefficients on the right-hand side of the equal sign in Eqs. (32) and (33) are known and those of the left-hand side are undetermined; the superscripts, e and o, denote the even part for $\cos(m\phi)$ and odd part for $\sin(m\phi)$, respectively. The matrices, $[SM_m^e]$ and $[SM_m^o]$, are shown below

$$[SM_0^e] = \begin{bmatrix} 2R^2(1 + ln\rho) + 2\rho^2 \ln\rho & -4R(1 + \ln\rho) \\ 2\frac{R^2}{\rho} + 2\rho(1 + 2\ln\rho) & \frac{-4R}{\rho} \end{bmatrix}, \quad m = 0 \tag{34}$$

$$[SM_1^e] = \begin{bmatrix} \rho(1 + 2\ln\rho) + \frac{3R^2}{2\rho} & -R\rho(1 + 2\ln\rho) - \frac{R^3}{2\rho} \\ (3 + 2\ln\rho) - \frac{3R^2}{2\rho^2} & -R(3 + 2ln\rho) + \frac{R^3}{2\rho^2} \end{bmatrix}, \quad m = 1 \tag{35}$$

$$[SM_m^e] = \begin{bmatrix} -(m-1)R^3 + (m+1)R\rho^2 & (m+2)(m-1)R^2 - m(m+1)\rho^2 \\ m(m-1)R^3 - (m-2)(m+1)R\rho^2 & -m(m+2)(m-1)R^2 + m(m+1)(m-2)\rho^2 \end{bmatrix}, \quad m = 2, 3, \ldots \tag{36}$$

$$[SM_1^o] = \begin{bmatrix} \rho(1 + 2\ln\rho) + \frac{3R^2}{2\rho} & -R\rho(1 + 2\ln\rho) - \frac{R^3}{2\rho} \\ (3 + 2\ln\rho) - \frac{3R^2}{2\rho^2} & -R(3 + 2\ln\rho) + \frac{R^3}{2\rho^2} \end{bmatrix}, \quad m = 1 \tag{37}$$

$$[SM_m^o] = \begin{bmatrix} -(m-1)R^3 + (m+1)R\rho^2 & (m+2)(m-1)R^2 - m(m+1)\rho^2 \\ m(m-1)R^3 - (m-2)(m+1)R\rho^2 & -m(m+2)(m-1)R^2 + m(m+1)(m-2)\rho^2 \end{bmatrix}, \quad m = 2, 3, ... \tag{38}$$

respectively. It is interesting to find that the coefficients of Eqs. (35) and (36) are the same to Eqs. (37) and (38), respectively. We determine the unknown coefficients by using the Eqs. (32) and (33). For the occurring mechanism of the degenerate scale, we examine the zero determinants for $[SM_m^e]$ and $[SM_m^o]$. In Eqs. (34), (36) and (38), the determinants of the three matrices are not zero for any value of a (Here, $R=\rho=a$). It is found that the zero determinants of influence matrices in Eqs. (35) and (37) occur in the direct BIEM ($\rho=R=a$) since

$$\det[SM_1^e]=\det[SM_1^o] = -16a^2(1+\ln(a))=0, \quad m=1. \tag{39}$$

As $(1+\ln a)$ becomes zero in Eq. (39), it indicates that the radius of value e^{-1} is the degenerate scale. In other words, we encounter the nonunique solution in mathematics because the matrices of $[SM_1^e]$ and $[SM_1^o]$ are singular.

Case 2. Simply-supported plate

For the simply-supported circular plate, the matrices $[SM_m^e]$ and $[SM_m^o]$ are obtained as

$$[SM_0^e]=\begin{bmatrix} R^2(1+\ln\rho)+\rho^2\ln\rho & 2(1+v)(1+\ln\rho) \\ R^2+\rho^2(1+2\ln\rho) & 2(1+v) \end{bmatrix}, \quad m=0 \tag{40}$$

$$[SM_1^e]=\begin{bmatrix} 2\rho^2(1+2\ln\rho)+R^2 & 2(3+v) \\ -2\rho^2R(3+2\ln\rho)+R^2 & 2(3+v) \end{bmatrix}, \quad m=1 \tag{41}$$

$$[SM_m^e]=\begin{bmatrix} \frac{-R^2}{m(m+1)}+\frac{\rho^2}{m(m-1)} & \frac{2(v+1)-m(v-1)}{m}+(1-v)\frac{\rho^2}{R^2} \\ \frac{R^2}{(m+1)\rho^2}-m(m+2)(m-1)R^2+m(m+1)(m-2)\rho^2 & \frac{(m(v-1)-2(v+1)))}{\rho^2}+\frac{(1-v)(-m+2)}{R^2} \end{bmatrix}, \quad m=2,3,\ldots \tag{42}$$

$$[SM_1^o]=\begin{bmatrix} 2\rho^2(1+2\ln\rho)+R^2 & 2(3+v) \\ -2\rho^2R(3+2\ln\rho)+R^2 & 2(3+v) \end{bmatrix}, \quad m=1 \tag{43}$$

$$[SM_m^o]=\begin{bmatrix} \frac{-R^2}{m(m+1)}+\frac{\rho^2}{m(m-1)} & \frac{2(v+1)-m(v-1)}{m}+(1-v)\frac{\rho^2}{R^2} \\ \frac{R^2}{(m+1)\rho^2}-m(m+2)(m-1)R^2+m(m+1)(m-2)\rho^2 & \frac{(m(v-1)-2(v+1)))}{\rho^2}+\frac{(1-v)(-m+2)}{R^2} \end{bmatrix}, \quad m=2,3,\ldots \tag{44}$$

respectively. The zero determinants of influence matrices in Eqs. (41) and (43) occur in the direct BIEM ($\rho=R=a$) since

$$16a^2(v+3)(1+\ln(a))=0, \quad m=1. \tag{45}$$

As $(1+\ln(a))$ becomes zero in Eq. (45), it means that the radius approaches the degenerate scale of e^{-1}.

Case 3. Free plate

Similarly, the matrices $[SM_m^e]$ and $[SM_m^o]$ are obtained as

$$[SM_0^e]=\begin{bmatrix} 4\pi(1+v)(1+\ln\rho) & 0 \\ 4\pi(1+v) & 0 \end{bmatrix}, \quad m=0 \tag{46}$$

$$[SM_1^e]=\begin{bmatrix} R & -1 \\ R & -1 \end{bmatrix}, \quad m=1 \tag{47}$$

$$[SM_m^e]=\begin{bmatrix} -\frac{m(v-1)-2(v+1)}{m}+(1-v)\frac{\rho^2}{R^2} & \frac{(m(1-v)-4)}{R}+m(1-v)\frac{\rho^2}{R^3} \\ \frac{m(v-1)-2(v+1)}{\rho}+(1-v)(-m+2)\frac{\rho}{R^2} & \frac{m(m(1-v)-4)}{R\rho}+m(-m+2)(1-v)\frac{\rho}{R^3} \end{bmatrix}, \quad m=2,3,\ldots \tag{48}$$

$$[SM_1^o]=\begin{bmatrix} R & -1 \\ R & -1 \end{bmatrix}, \quad m=1 \tag{49}$$

$$[SM_m^o]=\begin{bmatrix} -\frac{m(v-1)-2(v+1)}{m}+(1-v)\frac{\rho^2}{R^2} & \frac{(m(1-v)-4)}{R}+m(1-v)\frac{\rho^2}{R^3} \\ \frac{m(v-1)-2(v+1)}{\rho}+(1-v)(-m+2)\frac{\rho}{R^2} & \frac{m(m(1-v)-4)}{R\rho}+m(-m+2)(1-v)\frac{\rho}{R^3} \end{bmatrix}, \quad m=2,3,\ldots \tag{50}$$

respectively. By examining the zero determinants in Eqs. (46)–(50) for the free case, we find that there are no occurring mechanism of the degenerate scale but rigid body solution. It is easy to check that the zero determinant of matrices occur for any size of a since the row vectors in Eqs. (46), (47) and (49) are linearly dependent. The zero determinant results in rigid body modes instead of degenerate scales. The boundary densities, $m(s)$ and $v(s)$, are zeros due to free boundary condition. From the Eqs. (46), (47) and (49), we obtain the boundary eigenvector corresponding to the zero eigenvalue (multiplicity $= 3$) as

$$\left\{\begin{array}{c} a_0 \\ p_0 \\ a_1 \\ p_1 \\ \vdots \\ a_m \\ p_m \\ b_1 \\ q_1 \\ \vdots \\ b_m \\ q_m \end{array}\right\} = k_1 \left\{\begin{array}{c} 0 \\ 1 \\ 0 \\ 0 \\ \vdots \\ 0 \\ 0 \\ 0 \\ 0 \\ \vdots \\ 0 \\ 0 \end{array}\right\} + k_2 \left\{\begin{array}{c} 0 \\ 0 \\ 1 \\ a \\ \vdots \\ 0 \\ 0 \\ 0 \\ 0 \\ \vdots \\ 0 \\ 0 \end{array}\right\} + k_3 \left\{\begin{array}{c} 0 \\ 0 \\ 0 \\ 0 \\ \vdots \\ 0 \\ 0 \\ 1 \\ a \\ \vdots \\ 0 \\ 0 \end{array}\right\} \tag{51}$$

where k_1, k_2 and k_3 are the arbitrary coefficients. By substituting the series expansion in terms of degenerate kernel and boundary densities of Eq. (51) into the boundary integral equation of Eq. (12), we have the nontrivial potential $u(x)$

$$u(x) = u(\rho, \phi) = \text{constant}, \quad m = 0 \tag{52}$$

$$u(x) = u(\rho, \phi) = \frac{(1+v)}{4a}\rho\cos\phi, \quad m = 1 \tag{53}$$

$$u(x) = u(\rho, \phi) = \frac{(1+v)}{4a}\rho\sin\phi, \quad m = 1. \tag{54}$$

The zero determinant for the free case results in the three rigid body solutions of Eqs. (52), (53) and (54) for any value of a. All the degenerate scales for the three boundary conditions by using the six formulations are summarized in Table 1.

Table 1 Degenerate scales for different boundary in the continuous and discrete models using the boundary integral equation

Boundary condition	Clamped and Simply-supported	Free
Formulations		
u, θ formulation	$1 + \ln a = 0$	Never zero
u, m formulation	$\lfloor(\nu-1)(1+2\ln a) - 2(1+\nu)(1+\ln a)^2\rfloor [\nu + \nu\ln a - \ln a] = 0$	Never zero
u, v formulation	$(1+\ln a)(\nu - 4 - 2\ln a + 2\nu\ln a) = 0$	Never zero
θ, m formulation	$(1+\ln a)[\nu(1+\ln a) - \ln a - 2] = 0$	Never zero
θ, v formulation	$\nu(3 + 2\ln a) - 2\ln a = 0$	Never zero
m, v formulation	Never zero	Never zero

According to the results of the degenerate scale problem in the continuous model, we find that the same degenerate scales occur for the problems subject to the clamped and simply-supported boundary conditions and are mathematically realizable which means that the problem is uniquely solvable but the BIE has zero eigenvalue. For the free case, zero determinant results from zero eigenvalue due to the rigid body solution which is physically realizable. Since any two equations in the plate formulation (Eqs. (18)–(21)) can be chosen, $6(C_2^4)$ options of the formulation are considered. If we choose different formulae for either one of the the clamped, simply-supported or free circular cases, we find that the occurrence of the degenerate scale only depends on the formulation instead of the specified boundary condition. In other words, the clamped, simply-supported and free circular plates results in the same degenerate scale, once the same formulation is chosen.

2.3 Existence of the degenerate scale for a circular plate — discrete model (BEM)

Case 1. Clamped case

For the clamped case, Eqs. (22) and (23) can be rewritten as

$$\{f_1^c\} = [-U]\{v\} + [\Theta]\{m\}, \tag{55}$$

$$\{f_2^c\} = [-U_\theta]\{v\} + [\Theta_\theta]\{m\}. \tag{56}$$

By assembling Eqs. (55) and (56) together, we have

$$[SM^c]\left\{\begin{array}{c} v \\ m \end{array}\right\} = \left\{\begin{array}{c} f_1^c \\ f_2^c \end{array}\right\} \tag{57}$$

where

$$[SM^c] = \begin{bmatrix} -U & \Theta \\ -U_\theta & \Theta_\theta \end{bmatrix}_{4N\times 4N}. \tag{58}$$

Since the rotation symmetry is preserved for a circular boundary with uniform nodes, the influence matrices for the discrete model are found to be circulants. Therefore, we have the eigenvalues of $[SM^c]$,

$$\lambda^c = \begin{cases} 8\pi^2 a^4[1+\ln(a)+(\ln(a))^2], & l=0, \\ 4\pi^2 a^4[1+\ln(a)], & l=\pm 1, \\ -2\pi^2 a^4[\frac{1}{|l|(|l|-1)(|l|+1)^2}], & l=\pm 2,\pm 3,\ldots, \\ \pm(N-1),\pm N \end{cases} \tag{59}$$

According to the zero determinant of the $[SM^c]$ matrix, we examine the existence of the degenerate scales. For the case of $l = 0$ in Eq. (59), the term of $1 + \ln(a) + (\ln(a))^2$ is positive for any value of a. We obtain the possible degenerate scales and find the occurring mechanism of the degenerate scales in the discrete model by using the circulants for the circular plate. In the clamped case, we have the degenerate scale e^{-1} when $1 + \ln(a)$ approaches zero. The result of the Eq. (59) in the discrete model matches well with the Eq. (39) in the continuous model.

Case 2. Simply-supported case

For the simply-supported circular plate, we have the eigenvalues of $[SM^s]$ [32]

$$\lambda^s = \begin{cases} -8\pi^2 a^3(1+v)[1+2\ln(a) \\ \quad +2(\ln(a))^2], \quad l=0, \\ 4\pi^2 a^3(3+v)[1+\ln(a)], \quad l=\pm 1, \\ 4\pi^2 a^3[\frac{(|l|-2)(v(|l|-1)-(|l|+1))}{|l|^2(|l|-1)(|l|+1)}], \\ \quad l=\pm 2, \pm 3, \ldots, \pm(N-1), N \end{cases} \tag{60}$$

where the superscript "s" denotes the simply-supported case. By examining the zero determinant of the matrix $[SM^s]$, we obtain the possible degenerate scale of $1+\ln(a)$ in the discrete model when $l=\pm 1$. It is noted that the case of $l=0$ in Eq. (60) are always positive for any value of a due to the positive term of $1+2\ln(a)+2(\ln(a))^2$. We have the same degenerate scale of the clamped case by using the circulants for the circular plate. It indicates that the radius of e^{-1} is the degenerate scale. The result of the Eq. (60) in the discrete model matches well with the Eq. (45) in the continuous model.

Case 3. Free case

For the free circular plate, we have the eigenvalues of $[SM^f]$ [32]

$$\lambda^f = \begin{cases} 0, \quad l=0, \\ 0, \quad l=\pm 1, \\ 4\pi^2|l|^2(v-1)^2-4|l|v(v-1)+4(v^2-v-3), \\ l=\pm 2, \pm 3, \ldots, \pm(N-1), \pm N \end{cases} \tag{61}$$

By examining the determinant of matrix $[SM^f]$, we find that no degenerate scale but rigid body motion appears for the free case in the discrete model. It implies that we can solve the rigid body solution instead of worrying about the occurrence of the degenerate scale. For the cases of $l=0$ and $l=\pm 1$ in Eq. (61), the determinants are zero. In the clamped and simply-supported cases, there are no rigid body modes. For the free case, we may wonder why the three nontrivial modes exist in this case. The detailed discussions are addressed in Sect. 3. The result of the Eq. (61) in the discrete model matches well with the result of Eq. (51) in the continuous model. After comparing the results of continuous model with those of discrete model for the degenerate scale, good agreement is made. If we choose different formulae for either one of the clamped, simply-supported and free circular plate cases, we find that the occurrence of the degenerate scale only depends on the formulation instead of the boundary condition. It is interesting to find that the degenerate scale problem does not occur in the $m-v$ formulation. All the results are summarized in Table 1.

2.4 Discussion on nonuniqueness and relation of degenerate scale between the Laplace and biharmonic equations

The existence of nonuniqueness in the solution of boundary value problems (BVPs) by means of various integral representation can be categorized to three types. One is that the rigid body solution is imbedded in the boundary integral formulation for the Neumann or traction problem. Another kind of nonuniqueness appears in the plane BVP where a degenerate (critical) scale results in the zero eigenvalue of the influence matrix. The other kind of non-unique solutions occur when the hypersinglar or traction BIE is applied especially for multiply-connected problems.

Let us focus on the relation between the degenerate scale problem in the Laplace and biharmonic problems subject to different boundary conditions. For the Laplace problem, the phenomenon of degenerate scale, $\ln(a)=0$, occurs when using the singular (UT) formulation to solve the Dirichlet problem as shown in Fig. 2. The occurrence of the degenerate scale is mathematically realizable. But there are no degenerate scale for the Neumann problem when using the singular (UT) or hypersingular (LM) formulations. However, zero eigenvalue arises naturally due to the rigid body solution in physics. The outcome is physically realizable.

For the biharmonic problem, we have the six boundary integral equations for the plate subject to three kinds of boundary conditions. We find that the mechanism of degenerate scale of the clamped and simply-supported cases of biharmonic problems are similar to those of the Dirichlet problem of Laplace equation. By employing the boundary integral equations for the two boundary conditions, the former five approaches result in degenerate scales and the last one ($m-v$ formulation) does not have any degenerate scales for constrained problems. This fact agrees with the result that LM formulation can solve the Dirichlet problem of Laplace equation without any difficulty since the determinant of the influence matrix is never zero [9, 11, 13]. For the free case, the results are similar to the Neumann problem for the Laplace equation. It is noted that there is a rigid body solution for the Laplace problem subject to the Neumann boundary condition. On the other hand, we have three rigid body modes of the biharmonic problem for the free case in both the continuous and discrete models.

3. Discussions for the number of degenerate scales

In Sect. 2, we have demonstrated the existence of the degenerate scales which depends on the formulations instead of the boundary conditions. Chen et al. [9] have solved the degenerate scale problem for the Laplace equation successfully as shown in Fig. 2. Here, we discuss the number of the degenerate scales in each formulation for the clamped, simply-supported and free

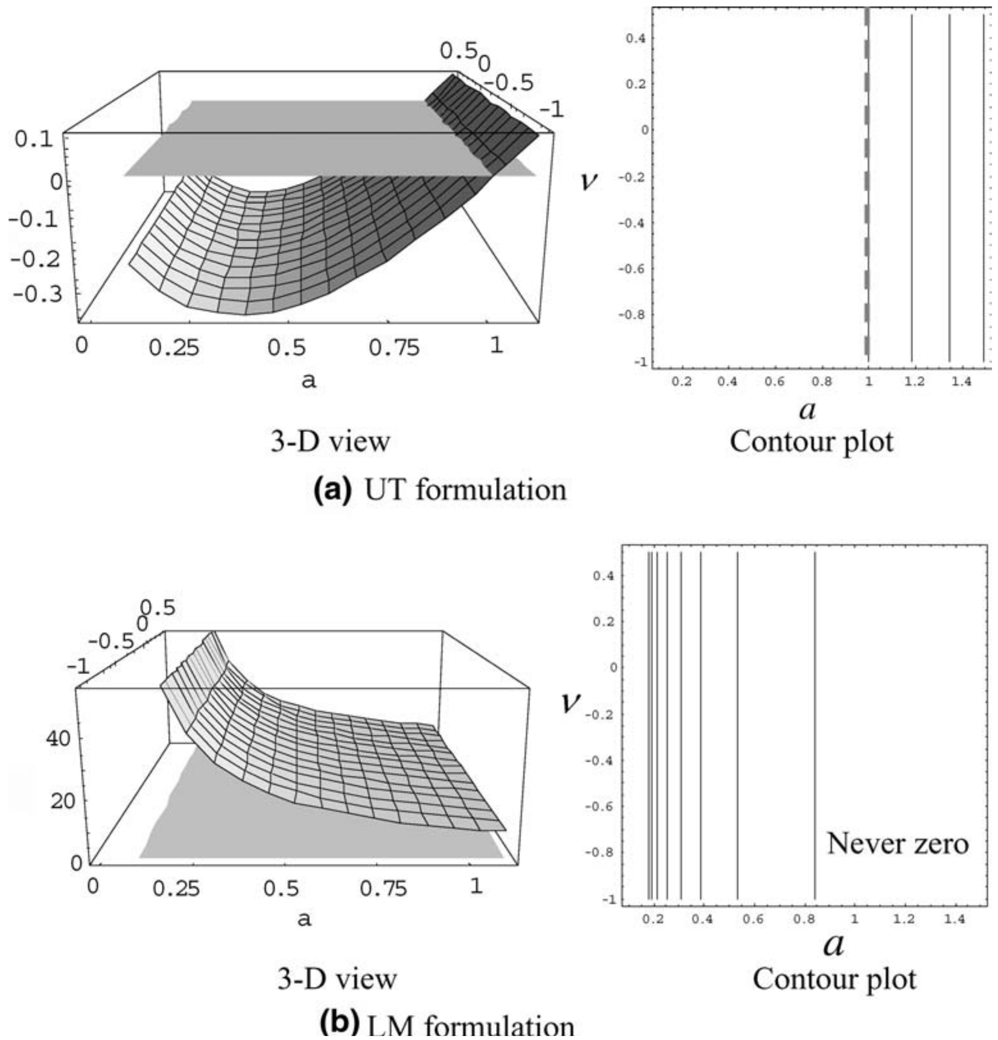

Fig. 2 3D and contour plots for the degenerate scale in the continuous and discrete models for the Laplace equation (The dotted line is the position that degenerate scales occur)

problems as shown in Table 1. We consider the damped and simply-supported problems together since no degenerate scale occurs in the free case. For the $u-\theta$ formulation, we have only one degenerate scale with the radius a which approaches e^{-1} $(1+\ln(a)=0)$ for any value of the Poisson ratio v. We plot the graphs of contour form and 3-D view for v $(-1<v\leq 0.5)$ and the radius a $(0<a<1.2)$ as shown in Fig. 3(a). Let us consider the contour plot of $u-m$ formulation, we may have two or three degenerate scales when v is fixed in Fig. 3(b). For the $u-v$ and $\theta-m$ formulations, we have one or two degenerate scales as shown in Figs. 3(c) and (d), respectively. By using the $\theta-v$ formulation, there is only one degenerate scale occurs when v is fixed in Fig. 3(e). No degenerate scale occurs in the $m-v$ formulation as shown in Table 2 and Fig. 3(f). It is obvious to find that we have at least one degenerate scale and have three at most when using the boundary element method except the $m-v$ formulation. Furthermore, we find that the occurring mechanism of degenerate scale depends on the Poisson ratio for the five formulations except $u-\theta$ formulation. Briefly speaking, the $m-v$ formulation is free of degenerate scale in sacrifice of using more complex kernels in a similar way of hypersingular formulation (LM equation) for the Laplace problem. From this study, we can predict the possible failure when using the BIEM/BEM to solve plate problems in advance.

4. Illustrative examples

Case 1:

According to the dual formulation, we use the null-field integral equations of Eqs. (18) and (21) to derive the analytical solution for the biharmonic problem in Fig. 4 [28] as follows:

$$\nabla^4 u(x)=0, x\in\Omega \tag{62}$$

subject to the essential boundary conditions

$$u(x)=0, x\in B \tag{63}$$

$$\frac{\partial u(x)}{\partial n}=\begin{cases}-1, \theta_0 & <\theta \quad <\theta_1 \\ 0, \theta_1 & <\theta \quad <2\pi+\theta_0\end{cases} \quad x\in B \tag{64}$$

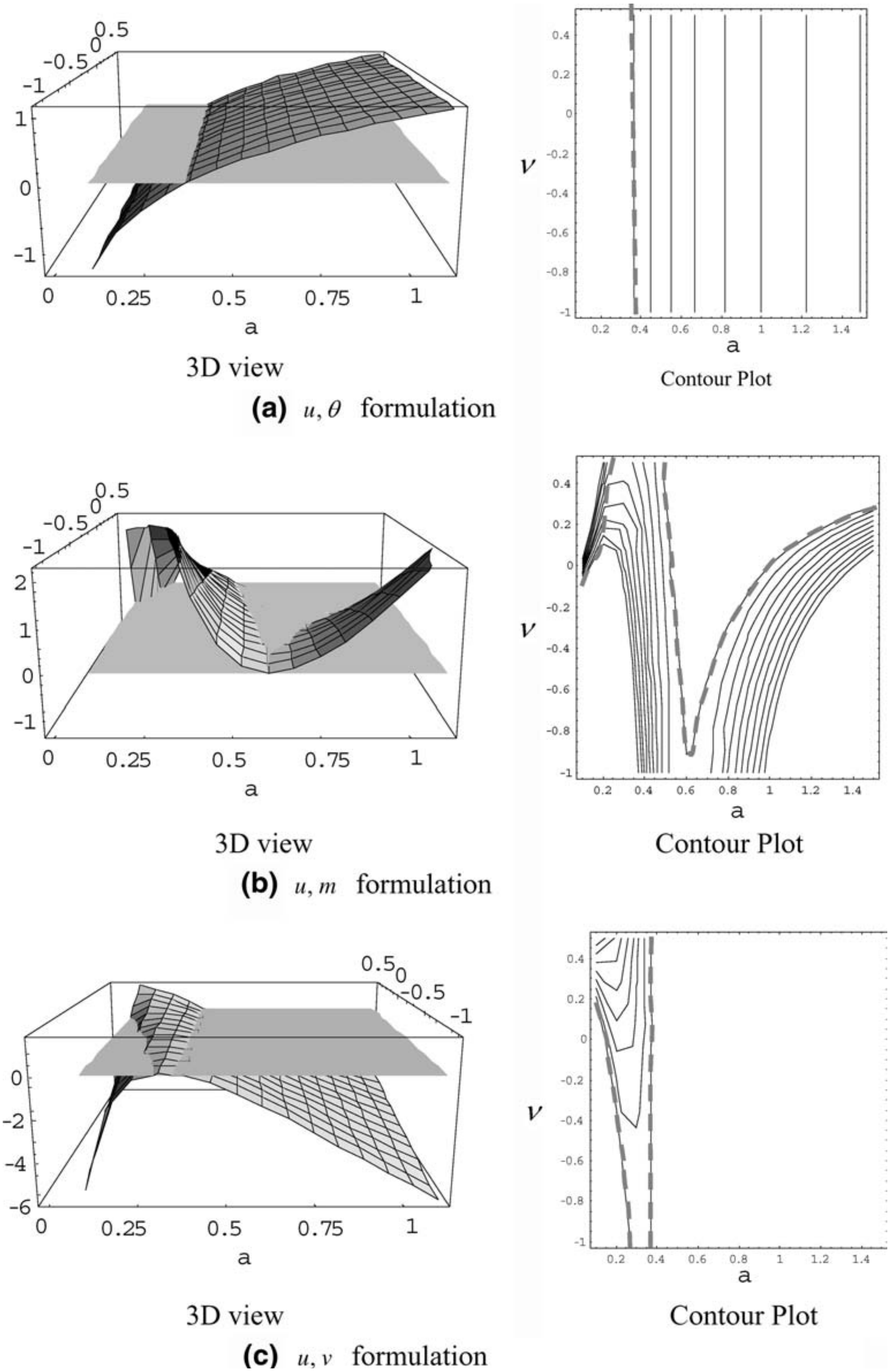

Fig. 3 3D-plot and contour for the degenerate scale in the continuous and discrete models of biharmonic equation using the boundary integral equations

where Ω is a circular domain with radius a. The boundary densities of $u(x)$ and $\frac{\partial u(x)}{\partial n}$ are expanded in terms of Fourier series

$$u(x) = g_0 + \sum_{m=1}^{\infty}(g_m \cos(m\phi) + h_m \sin(m\phi)), \tag{65}$$

$$\frac{\partial u(x)}{\partial n} = g_0^* + \sum_{m=1}^{\infty}(g_m^* \cos(m\phi) + h_m^* \sin(m\phi)), \tag{66}$$

where the specified Fourier coefficients are

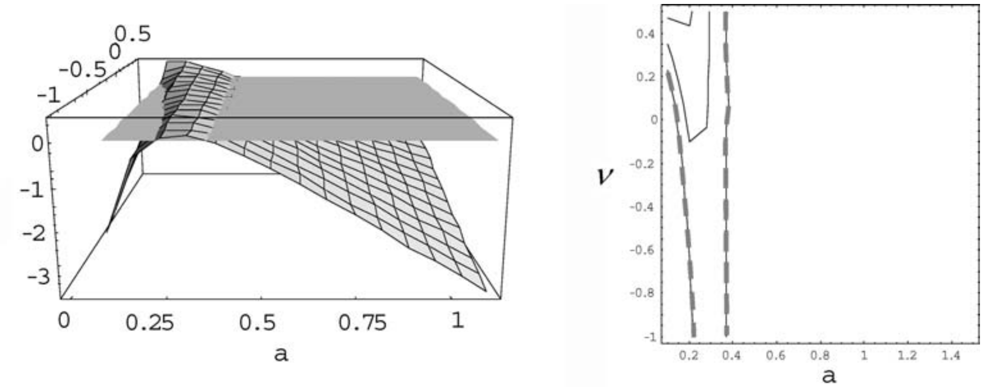

3D view

Contour Plot

(d) θ, m formulation

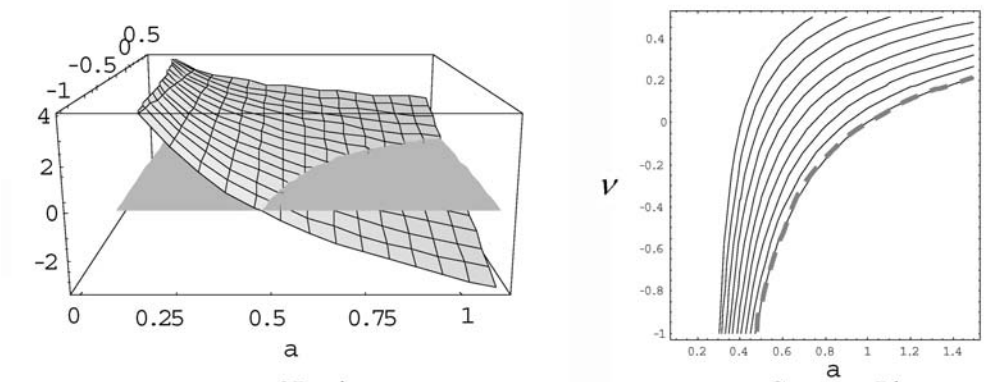

3D view

Contour Plot

(e) θ, v formulation

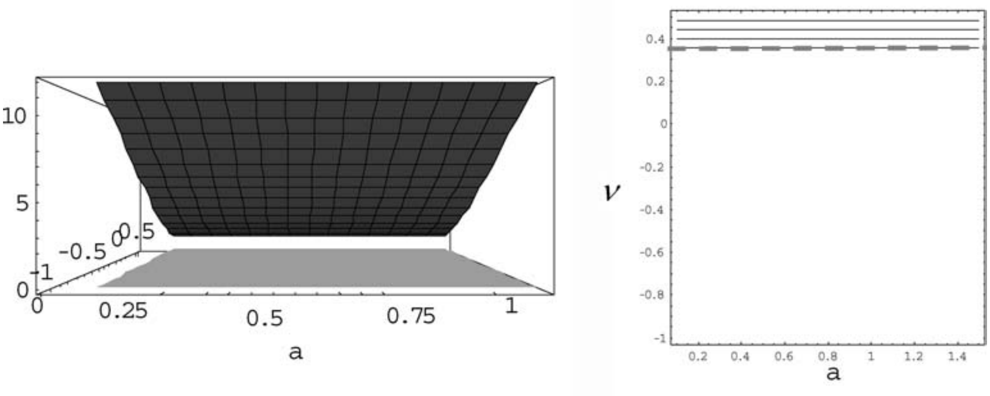

3D view

Contour Plot

(f) m, v formulation

Fig. 3 (Contd.)

$$g_0 = g_m = h_m = 0, \quad g_0^* = \frac{1}{2\pi}(\theta_1 - \theta_0),$$
$$g_m^* = \frac{1}{m\pi}(\sin m\theta_1 - \sin m\theta_0), \quad h_m^* = \frac{1}{m\pi}(\cos m\theta_1 - \cos m\theta_0). \tag{67}$$

By utilizing the null-field integral equation in conjunction with Fourier series and the series expansion in terms of degenerate kernels for fundamental solutions, we can derive the series solution. For simplicity, we choose $\theta_0 = \frac{\pi}{2}$ and $\theta_1 = \frac{-\pi}{2}$. By substituting the density functions of Eqs. (26) and (27) and expanding the fundamental solution in terms of degenerate kernel into the null-field integral equations, $u - \theta$ formulation, the Fourier

Table 2 Relationship between the Laplace problem and biharmonic problem

	Laplace problem				Biharmonic problem												
Governing equation	$\nabla^2 u(x) = 0$				$\nabla^4 u(x) = 0$												
Fundamental solution	$U(s,x) = \ln(r)$				$U(s,x) = r^2 \ln(r)$												
Boundary condition	**Dirichlet**		Neumann		Clamped						Simply-supported						Free
Formulation	UT	LM	UT	LM	$C_2^4 = 6$ options						$C_2^4 = 6$ options						$C_2^4 = 6$ options
					$u-\theta$	$u-m$	$u-v$	$\theta-m$	$\theta-v$	$m-v$	$u-\theta$	$u-m$	$u-v$	$\theta-m$	$\theta-v$	$m-v$	
Degenerate scale	$\ln(a) = 0$	NA	NA		See Table 3-3					NA	See Table 3-4					NA	NA
Nontrivial mode	Mathematical realizable (spurious mode)	OK	Physically realizable (Rigid body mode)		Mathematically realizable (spurious mode)					OK	Mathematically realizable (spurious modes)					OK	Physically realizable (Rigid body modes)

coefficients for $m(s)$ and $v(s)$ in Eqs. (18) and (19) are obtained as shown below:

$$p_0 = \frac{-(1+v)}{2a}, \tag{68}$$

$$p_1 = \frac{-2(v+3)}{\pi a}, \tag{69}$$

$$p_m = \frac{-2(1+2m+v)}{m\pi a} \sin\frac{m\pi}{2}, m = 2, 3, \ldots \tag{70}$$

$$a_0 = 0, \tag{71}$$

$$a_1 = \frac{-2(v+3)}{\pi a^2}, \tag{72}$$

$$a_m = \frac{-2(2+2m+mv)}{\pi a^2} \sin\frac{m\pi}{2}, \quad m = 2, 3, \ldots. \tag{73}$$

After obtaining the boundary densities, we substitute them into the boundary integral equations to yield the series solution

$$u(\rho,\phi) = \frac{1}{8\pi}\{2\pi(a - \frac{\rho^2}{a}) + \sum_{m=1}^{\infty} \frac{8\rho^m(a^2-\rho^2)}{ma^{m+1}} \sin\frac{m\pi}{2} \cos(m\phi)\}. \tag{74}$$

For purpose of comparison, the series solution can also be derived by using the Trefftz method as follows [15]:

$$u(x) = a_0 + b_0\rho^2 + \sum_{m=1}^{\infty}(c_m\rho^m\cos(m\phi) + d_m\rho^m\sin(m\phi)) + \sum_{m=1}^{\infty}(g_m\rho^{m+2}\cos(m\phi) + h_m\rho^{m+2}\sin(m\phi)), \tag{75}$$

$$\frac{\partial u(x)}{\partial n_x} = 2b\rho + \sum_{m=1}^{\infty} m(c_m\rho^{m-1}\cos(m\phi) + d_m\rho^{m-1}\sin(m\phi)) + \sum_{m=1}^{\infty}(m+2)(g_m\rho^{m+1}\cos(m\phi) + h_m\rho^{m+1}\sin(m\phi)), \tag{76}$$

where the a, b, c_m, d_m, g_m and h_m are the unknown coefficients. By substituting Eqs. (75) and (76) into the boundary condition of Eq. (63), the unknown coefficients are obtained as

$$a_0 = \frac{1}{4}, \tag{77}$$

$$b_0 = \frac{-1}{4}, \tag{78}$$

$$c_m = \frac{1}{m\pi}\cos(m\pi)\sin(\frac{m\pi}{2}), \tag{79}$$

$$g_m = \frac{-1}{m\pi}\cos(m\pi)\sin(\frac{m\pi}{2}), \tag{80}$$

$$d_m = h_m = 0. \tag{81}$$

We have the field solution as follows:

$$u(x) = u(\rho,\phi) = \frac{1}{4}(1-\rho^2) - \sum_{m=1}^{\infty}\frac{1}{m\pi}\cos(m\pi)\sin\left(\frac{m\pi}{2}\right)(\rho^{m+2}\cos(m\phi) - \rho^m\cos(m\phi)). \tag{82}$$

Eq. (82) are found to be the same to Eq. (74). It is interesting to find that the six Trefftz bases are all imbedded in the series expansion in terms of degenerate kernel for fundamental soluitons [15]. The exact solution was obtained in a different way by Mills [28] as follows:

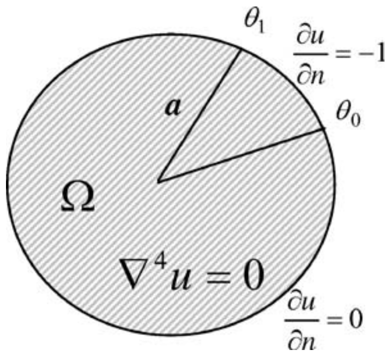

Fig. 4 The chart of the biharmonic equation with the essential boundary condition (Case 1)

$$u(r,\theta) = \frac{1}{2\pi}(1-r^2)\left[\gamma + \arctan\left(\frac{1+r}{1-r}\tan\left(\frac{\theta_1-\theta}{2}\right)\right) - \arctan\left(\frac{1+r}{1-r}\tan\left(\frac{\theta_0-\theta}{2}\right)\right)\right] \tag{83}$$

Fig. 5 Contour plots of biharmonic fields using degenerate kernels and null-field integral equation

where

$$\gamma = \begin{cases} 0, \theta_1 - \pi < \theta < \theta_0 + \pi \\ \pi, \theta_0 + \pi < \theta < \theta_1 + \pi. \end{cases} \tag{84}$$

We plot the results by using 20, 50 and 100 terms of the series-form solution of Eq. (74) and find that the series solution coverges well to the exact solution of Eq. (83) as shown in Figs. 5(a), (b), (c) and (d). It deserves to be mentioned that the degenerate scale occurs when $1 + \ln(a) = 0$ in the continuous and discrete models using the $u-\theta$ formulation. In this case, we do not observe the occurrence of the degenerate scale due to the zero coefficient of $a_0 = \frac{g_0}{1+ln(a)}$ in Eq. (71) when $m = 0$ even though $a = e^{-1}$. That is to say, we are fortunate to solve the problem free of encountering the degenerate scale problem due to the zero participation factor for the spurious mode [14].

Case 2:

Let us consider the biharmonic problem subject to the essential boundary condition as shown in Fig. 6

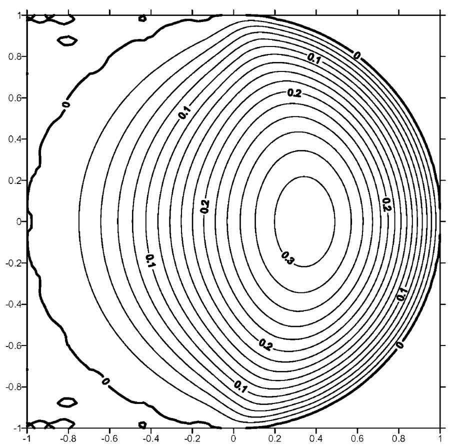

(a) BIEM (M=20)

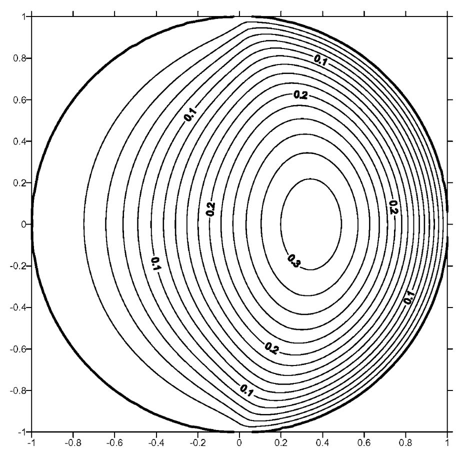

(b) BIEM (M=50)

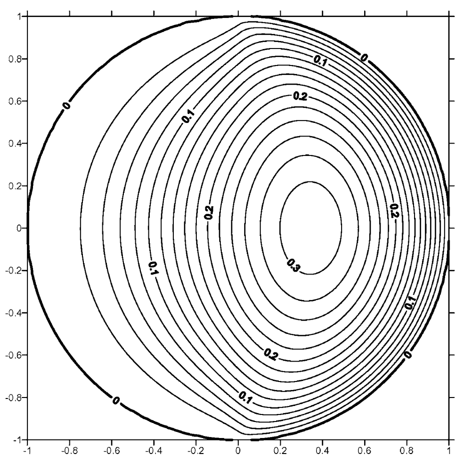

(c) BIEM (M=100)

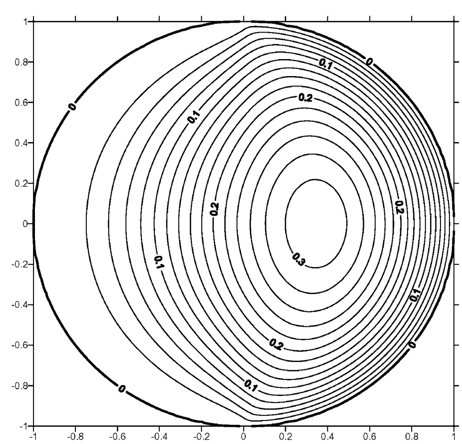

(d) Exact solution

$$u(x) = \begin{cases} \frac{\theta-\alpha}{\epsilon_1} + 1, \alpha - \epsilon_1 < \theta < \alpha + \epsilon_1 \\ 2, \alpha + \epsilon_1 < \theta < \beta - \epsilon \\ \frac{\beta-\theta}{\epsilon} + 1, \beta - \epsilon < \theta < \beta + \epsilon \\ 0, \beta + \epsilon < \theta < \alpha - \epsilon_1 \end{cases} \tag{85}$$

$$\frac{\partial u(x)}{\partial n} = 0, \tag{86}$$

$$\begin{bmatrix} \rho(1+2\ln\rho) + \frac{3R^2}{2\rho} & -R\rho(1+2\ln\rho) - \frac{R^3}{2\rho} \\ (3+2\ln\rho) - \frac{3R^2}{2\rho^2} & -R(3+2\ln\rho) + \frac{R^3}{2\rho^2} \end{bmatrix} \begin{Bmatrix} a_1 \\ p_1 \end{Bmatrix} = \begin{Bmatrix} 0 \\ 0 \end{Bmatrix}, \tag{88}$$

$$\begin{bmatrix} -(m-1)R^3 + (m+1)R\rho^2 & (m+2)(m-1)R^2 - m(m+1)\rho^2 \\ m(m-1)R^3 - (m-2)(m+1)R\rho^2 & -m(m+2)(m-1)R^2 + m(m+1)(m-2)\rho^2 \end{bmatrix} \begin{Bmatrix} a_m \\ p_m \end{Bmatrix} = \begin{Bmatrix} 0 \\ 0 \end{Bmatrix}, m = 2, 3, \ldots. \tag{89}$$

We choose $\alpha = \frac{\pi}{8}$, $\beta = \pi$, $\epsilon = \epsilon_1 = \frac{\pi}{32}$. By using the null-field integral equation ($u - \theta$ formulation) in conjunction with the series expansion in terms of degenerate kernel, we have

$$\begin{bmatrix} 2R^2(1+\ln\rho) + 2\rho^2\ln\rho & -4R(1+\ln\rho) \\ 2\frac{R^2}{\rho} + 2\rho(1+2\ln\rho) & \frac{-4R}{\rho} \end{bmatrix} \begin{Bmatrix} a_0 \\ p_0 \end{Bmatrix} = \begin{Bmatrix} 0 \\ 0 \end{Bmatrix}, \tag{87}$$

For simplicity, the Poisson ratio is assumed to be $v = 0.3$. In Eq. (88), we find the occurrence of the degenerate scale when the radius a approaches e^{-1} $(1 + \ln(a) = 0)$ using the $u - \theta$ formulation. Similarly, the occurrence of degenerate scale when using the other five formulations is shown in Fig. 7. Good agreement is made.

5. Conclusions

In this paper, we employed the null-field integral equation in conjunction with Fourier series and the series expansion in terms of degenerate kernel for fundamental

Fig. 6 Biharmpnic problem (Case 2)

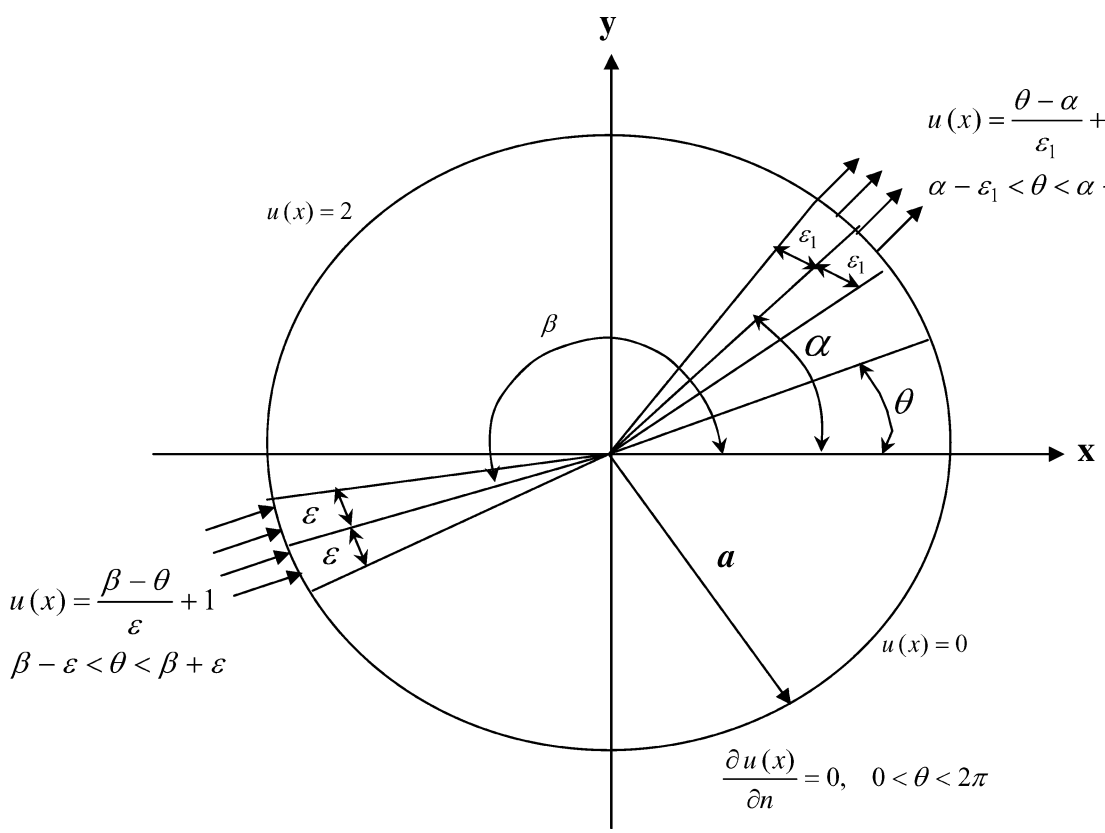

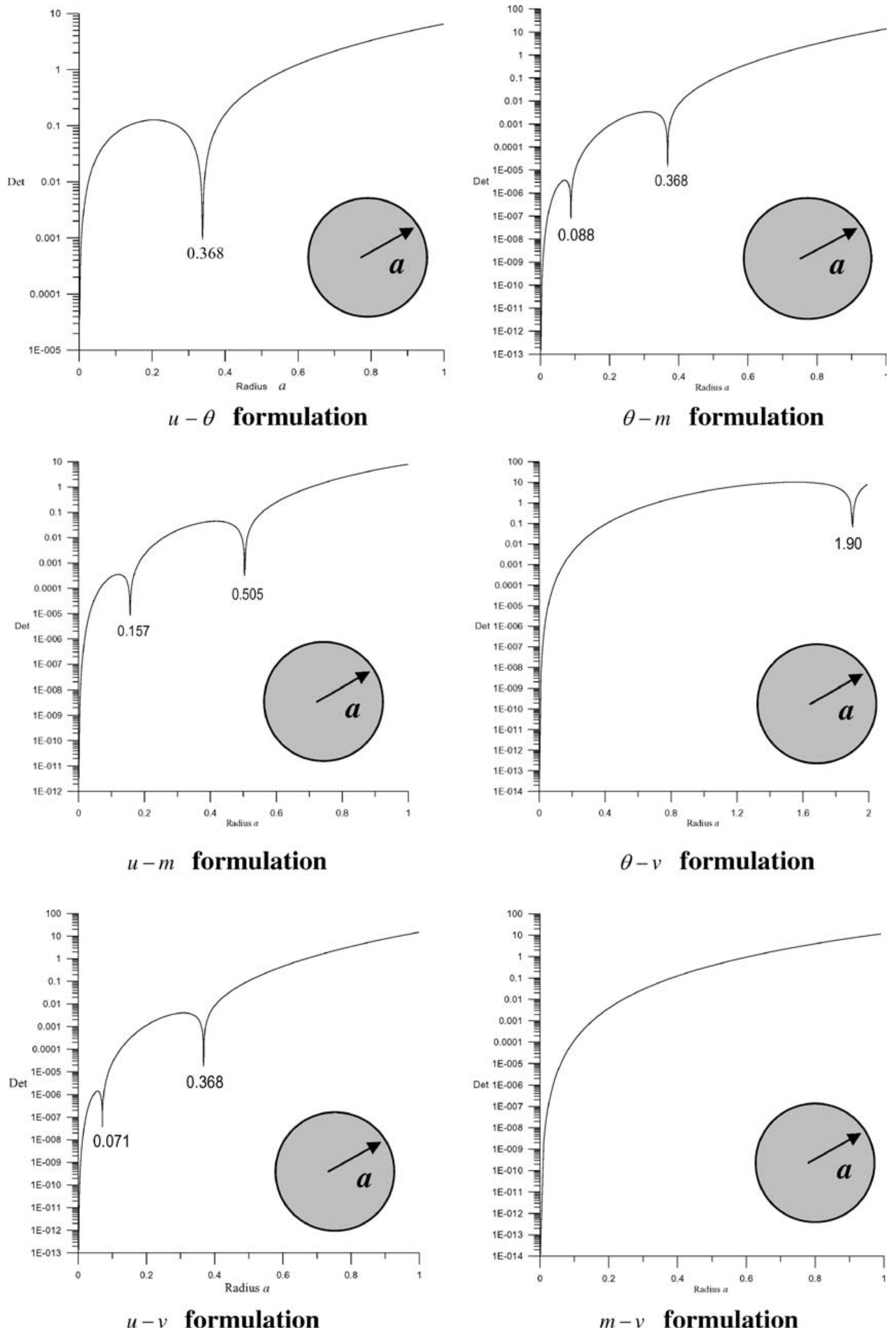

Fig. 7 Determinant versus the radius a using the BIEM/BEM for a circular plate problem ($\nu = 0.3$)

solutions to derive the degenerate scales of plate problem for the circular plate. The continuous and discrete models were both considered by using the direct BIEM (continuous model) and direct BEM (discrete model), respectively.

The occurrence of degenerate scales not only depends on the formulation that we choose but also on the Poisson's ratio. The degenerate scales of the Laplace and biharmonic problems are also compared with. We have only one rigid body mode of Laplace equation when using the *UT* or *LM* formulation for the Neumann problem but have three rigid body modes of bihamonic equation using the six boundary integral formulations for the free problem. Futhermore, we have determined the number of degenerate scales in each formulation. For the former five boundary integral formulations, we have at least one degenerate scale and have three at most. Regarding to the $m-v$ formulation, the degenerate scales disappear for constrained problems but rigid body modes are present for free problems. That is to say, we can adopt it to solve the biharmonic equation without any risk of degenerate scales in sacrifice of more complex kernels.

Appendix A Degenerate kernels for the sixteen kernel functions

$$U(s,x)=\begin{cases} U^I(s,x)=\rho^2(1+\ln R)+R^2\ln R-R\rho(1+2\ln R) \\ \cos(\theta-\phi)-\sum\limits_{m=1}^{\infty}\frac{1}{m(m+1)}\frac{\rho^{m+2}}{R^m}\cos[m(\theta-\phi)] \\ +\sum\limits_{m=2}^{\infty}\frac{1}{m(m-1)}\frac{\rho^m}{R^{m-2}}\cos[m(\theta-\phi)],R\geq\rho \\ U^E(s,x)=R^2(1+\ln\rho)+\rho^2\ln\rho \\ -\rho R(1+2\ln\rho)\cos(\theta-\phi) \\ -\sum\limits_{m=1}^{\infty}\frac{1}{m(m+1)}\frac{R^{m+2}}{\rho^m}\cos[m(\theta-\phi)] \\ +\sum\limits_{m=2}^{\infty}\frac{1}{m(m-1)}\frac{R^m}{\rho^{m-2}}\cos[m(\theta-\phi)],\rho>R \end{cases}$$

$$U_\theta(s,x)=\begin{cases} U_\theta^I(s,x)=2\rho(1+\ln R)-R(1+2\ln R) \\ \cos(\theta-\phi)-\sum\limits_{m=1}^{\infty}\frac{m+2}{m(m+1)}\frac{\rho^{m+1}}{R^m}\cos[m(\theta-\phi)] \\ +\sum\limits_{m=2}^{\infty}\frac{1}{m-1}\frac{\rho^{m-1}}{R^{m-2}}\cos[m(\theta-\phi)],R\geq\rho \\ U_\theta^E(s,x)=\frac{R^2}{\rho}+\rho(1+2\ln\rho) \\ -R(3+2\ln\rho)\cos(\theta-\phi) \\ +\sum\limits_{m=1}^{\infty}\frac{1}{m+1}\frac{R^{m+2}}{\rho^{m+1}}\cos[m(\theta-\phi)] \\ -\sum\limits_{m=2}^{\infty}\frac{m-2}{m(m-1)}\frac{R^m}{\rho^{m-1}}\cos[m(\theta-\phi)],\rho>R \end{cases}$$

$$U_m(s,x)=\begin{cases} U_m^I(s,x)=2(1+v)(1+\ln R) \\ +\sum\limits_{m=1}^{\infty}\frac{m(v-1)-2(v+1)}{m}\frac{\rho^m}{R^m}\cos[m(\theta-\phi)] \\ +\sum\limits_{m=2}^{\infty}(1-v)\frac{\rho^{m-2}}{R^{m-2}}\cos[m(\theta-\phi)],R>\rho \\ U_m^E(s,x)=\frac{R^2}{\rho^2}(v-1)+(3+2\ln\rho) \\ +v(1+2\ln\rho)-\frac{2R}{\rho}(1+v)\cos(\theta-\phi) \\ +\sum\limits_{m=1}^{\infty}(v-1)\frac{R^{m+2}}{\rho^{m+2}}\cos[m(\theta-\phi)] \\ +\sum\limits_{m=2}^{\infty}\frac{m(1-v)-2(1+v)}{m}\frac{R^m}{\rho^m}\cos[m(\theta-\phi)],\rho>R \end{cases}$$

$$U_v(s,x)=\begin{cases} U_v^I(s,x)=\sum\limits_{m=1}^{\infty}(m-4-mv)\frac{\rho^{m-1}}{R^m}\cos[m(\theta-\phi)] \\ +\sum\limits_{m=2}^{\infty}m(1-v)\frac{\rho^{m-3}}{R^{m-2}}\cos[m(\theta-\phi)],R>\rho \\ U_v^E(s,x)=\frac{4}{\rho}+\sum\limits_{m=1}^{\infty}m(v-1)\frac{R^{m+2}}{\rho^{m+3}}\cos[m(\theta-\phi)] \\ +\sum\limits_{m=2}^{\infty}(-mv+m+4)\frac{R^m}{\rho^{m+1}}\cos[m(\theta-\phi)],\ \rho>R \end{cases}$$

$$\Theta(s,x)=\begin{cases} \Theta^I(s,x)=\frac{\rho^2}{R}+R(1+2\ln R)-\rho(3+2\ln R) \\ \cos(\theta-\phi)+\sum\limits_{m=1}^{\infty}\frac{1}{m+1}\frac{\rho^{m+2}}{R^{m+1}}\cos[m(\theta-\phi)] \\ -\sum\limits_{m=2}^{\infty}\frac{m-2}{m(m-1)}\frac{\rho^m}{R^{m-1}}\cos[m(\theta-\phi)],R\geq\rho \\ \Theta^E(s,x)=2R(1+\ln\rho)-\rho(1+2\ln\rho) \\ \cos(\theta-\phi)-\sum\limits_{m=1}^{\infty}\frac{m+2}{m(m+1)}\frac{R^{m+1}}{\rho^m}\cos[m(\theta-\phi)] \\ +\sum\limits_{m=2}^{\infty}\frac{1}{m-1}\frac{R^{m-1}}{\rho^{m-2}}\cos[m(\theta-\phi)],\rho>R \end{cases}$$

$$\Theta_\theta(s,x)=\begin{cases} \Theta_\theta^I(s,x)=\frac{2\rho}{R}-(3+2\ln R)\cos(\theta-\phi) \\ +\sum\limits_{m=1}^{\infty}\frac{m+2}{m+1}\frac{\rho^{m+1}}{R^{m+1}}\cos[m(\theta-\phi)] \\ -\sum\limits_{m=2}^{\infty}\frac{m-2}{m-1}\frac{\rho^{m-1}}{R^{m-1}}\cos[m(\theta-\phi)],R\geq\rho \\ \Theta_\theta^E(s,x)=\frac{2R}{\rho}-(3+2\ln\rho)\cos(\theta-\phi) \\ +\sum\limits_{m=1}^{\infty}\frac{m+2}{m+1}\frac{R^{m+1}}{\rho^{m+1}}\cos[m(\theta-\phi)] \\ -\sum\limits_{m=2}^{\infty}\frac{m-2}{m-1}\frac{R^{m-1}}{\rho^{m-1}}\cos[m(\theta-\phi)],\rho>R \end{cases}$$

$$\Theta_m(s,x)=\begin{cases} \Theta_m^I(s,x)=\frac{2}{R}(1+v)-\sum\limits_{m=1}^{\infty}[m(v-1) \\ -2(v+1)]\frac{\rho^m}{R^{m+1}}\cos[m(\theta-\phi)] \\ -\sum\limits_{m=2}^{\infty}(1-v)(m-2)\frac{\rho^{m-2}}{R^{m-1}}\cos[m(\theta-\phi)], \\ R>\rho \\ \Theta_m^E(s,x)=\frac{2R}{\rho^2}(v-1)-\frac{2}{\rho}(1+v)\cos(\theta-\phi) \\ +\sum\limits_{m=1}^{\infty}(m+2)(v-1)\frac{R^{m+1}}{\rho^{m+2}}\cos[m(\theta-\phi)] \\ +\sum\limits_{m=2}^{\infty}[m(1-v)-2(1+v)]\frac{R^{m-1}}{\rho^m} \\ \cos[m(\theta-\phi)],\rho>R \end{cases}$$

$$\Theta_v(s,x)=\begin{cases}\Theta_v^I(s,x)=-\sum_{m=1}^{\infty}m(m-4-mv)\frac{\rho^{m-1}}{R^{m+1}}\\ \quad\cos[m(\theta-\phi)]-\sum_{m=2}^{\infty}m(m-2)(1-v)\\ \quad\frac{\rho^{m-3}}{R^{m-1}}\cos[m(\theta-\phi)],R>\rho\\ \Theta_v^E(s,x)=\sum_{m=1}^{\infty}m(m+2)(v-1)\frac{R^{m+1}}{\rho^{m+3}}\\ \quad\cos[m(\theta-\phi)]+\sum_{m=2}^{\infty}m(-mv+m+4)\\ \quad\frac{R^{m-1}}{\rho^{m+1}}\cos[m(\theta-\phi)],\rho>R\end{cases}$$

$$M(s,x)=\begin{cases}M^I(s,x)=(v-1)\frac{\rho^2}{R^2}+(v+3)+2(v+1)\\ \quad\ln\,R-(v+1)\frac{2\rho}{R}\cos(\theta-\phi)+\sum_{m=1}^{\infty}(v-1)\\ \quad\frac{\rho^{m+2}}{R^{m+2}}\cos[m(\theta-\phi)]+\sum_{m=2}^{\infty}\frac{m(1-v)-2(1+v)}{m}\frac{\rho^m}{R^m}\\ \quad\cos[m(\theta-\phi)],R\geq\rho\\ M^E(s,x)=2(1+v)(1+\ln\,\rho)\\ \quad+\sum_{m=1}^{\infty}\frac{m(v-1)-2(v+1)}{m}\frac{R^m}{\rho^m}\cos[m(\theta-\phi)]\\ \quad+\sum_{m=2}^{\infty}(1-v)\frac{R^{m-2}}{\rho^{m-2}}\cos[m(\theta-\phi)],\rho>R\end{cases}$$

$$M_\theta(s,x)=\begin{cases}M_\theta^I(s,x)=\frac{2\rho(v-1)}{R^2}-\frac{2(v+1)}{R}\cos(\theta-\phi)\\ \quad+\sum_{m=1}^{\infty}(v-1)(m+2)\frac{\rho^{m+1}}{R^{m+2}}\cos[m(\theta-\phi)]\\ \quad+\sum_{m=2}^{\infty}[m(1-v)-2(1+v)]\frac{\rho^{m-1}}{R^m}\\ \quad\cos[m(\theta-\phi)],R>\rho\\ M_\theta^E(s,x)=\frac{2(1+v)}{\rho}-\sum_{m=1}^{\infty}(m(v-1)\\ \quad-2(v+1))\frac{R^m}{\rho^{m+1}}\cos[m(\theta-\phi)]+\sum_{m=2}^{\infty}[(1-v)\\ \quad(-m+2)]\frac{R^{m-2}}{\rho^{m-1}}\cos[m(\theta-\phi)],\rho>R\end{cases}$$

$$M_m(s,x)=\begin{cases}M_m^I(s,x)=\frac{2(v^2-1)}{R^2}+\sum_{m=1}^{\infty}[m(v-1)-2(v+1)]\\ \quad(m+1)(1-v)\frac{\rho^m}{R^{m+2}}\cos[m(\theta-\phi)]\\ \quad+\sum_{m=2}^{\infty}(1-v)(m-1)[m(1-v)-2(v+1)]\\ \quad\frac{\rho^{m-2}}{R^m}\cos[m(\theta-\phi)],R\geq\rho\\ M_m^E(s,x)=\frac{2(v^2-1)}{\rho^2}+\sum_{m=1}^{\infty}[m(v-1)\\ \quad-2(v+1)](m+1)(1-v)\frac{R^m}{\rho^{m+2}}\\ \quad\cos[m(\theta-\phi)]+\sum_{m=2}^{\infty}(1-v)(m-1)\\ \quad[m(1-v)-2(v+1)]\frac{R^{m-2}}{\rho^m}\cos[m(\theta-\phi)],\\ \quad\rho>R\end{cases}$$

$$M_v(s,x)=\begin{cases}M_v^I(s,x)=\sum_{m=1}^{\infty}m(m+1)(1-v)[m(1-v)\\ \quad-4]\frac{\rho^{m-1}}{R^{m+2}}\cos[m(\theta-\phi)]+\sum_{m=2}^{\infty}(1-v)\\ \quad m(m-1)[m(1-v)-2(1+v)]\frac{\rho^{m-3}}{R^m}\\ \quad\cos[m(\theta-\phi)],R>\rho\\ M_v^E(s,x)=\sum_{m=1}^{\infty}m(m+1)(1-v)[m(v-1)\\ \quad-2(v+1)]\frac{R^m}{\rho^{m+3}}\cos[m(\theta-\phi)]+\sum_{m=2}^{\infty}(1-v)\\ \quad m(m-1)[m(1-v)+4]\frac{R^{m-2}}{\rho^{m+1}}\cos[m(\theta-\phi)],\\ \quad\rho>R\end{cases}$$

$$V(s,x)=\begin{cases}V^I(s,x)=\frac{4}{R}+\sum_{m=1}^{\infty}m(v-1)\frac{\rho^{m+2}}{R^{m+3}}\cos[m(\theta-\phi)]\\ \quad+\sum_{m=2}^{\infty}(m+4-mv)\frac{\rho^m}{R^{m+1}}\cos[m(\theta-\phi)],R>\rho\\ V^E(s,x)=\sum_{m=1}^{\infty}[m(1-v)-4]\frac{R^{m-1}}{\rho^m}\\ \quad\cos[m(\theta-\phi)]+\sum_{m=2}^{\infty}m(1-v)\frac{R^{m-3}}{\rho^{m-2}}\\ \quad\cos[m(\theta-\phi)],\rho>R\end{cases}$$

$$V_\theta(s,x)=\begin{cases}V_\theta^I(s,x)=\sum_{m=1}^{\infty}m(m+2)(v-1)\frac{\rho^{m+1}}{R^{m+3}}\\ \quad\cos[m(\theta-\phi)]+\sum_{m=2}^{\infty}m(m+4-mv)\frac{\rho^{m-1}}{R^{m+1}}\\ \quad\cos[m(\theta-\phi)],R>\rho\\ V_\theta^E(s,x)=-\sum_{m=1}^{\infty}m[m(1-v)-4]\frac{R^{m-1}}{\rho^{m+1}}\\ \quad\cos[m(\theta-\phi)]+\sum_{m=2}^{\infty}m(-m+2)(1-v)\frac{R^{m-3}}{\rho^{m-1}}\\ \quad\cos[m(\theta-\phi)],\rho>R\end{cases}$$

$$V_m(s,x)=\begin{cases}V_m^I(s,x)=\sum_{m=1}^{\infty}m(m+1)(1-v)[m(v-1)\\ \quad-2(v+1)]\frac{\rho^m}{R^{m+3}}\cos[m(\theta-\phi)]\\ \quad+\sum_{m=2}^{\infty}m(m-1)(1-v)[m(1-v)+4]\frac{\rho^{m-2}}{R^{m+1}}\\ \quad\cos[m(\theta-\phi)],R>\rho\\ V_m^E(s,x)=\sum_{m=1}^{\infty}m(m+1)(1-v)[m(1-v)\\ \quad-4]\frac{R^{m-1}}{\rho^{m+2}}\cos[m(\theta-\phi)]+\sum_{m=2}^{\infty}m(m-1)\\ \quad(1-v)[m(1-v)-2(v+1)]\frac{R^{m-3}}{\rho^m}\\ \quad\cos[m(\theta-\phi)],\rho>R\end{cases}$$

$$V_v(s,x)=\begin{cases} V_v^I(s,x)=\sum_{m=1}^{\infty} m^2(m+1)(1-v)[m(1-v) \\ \quad -4]\frac{\rho^{m-1}}{R^{m+3}}\cos[m(\theta-\phi)]+\sum_{m=2}^{\infty} m^2(m-1) \\ \quad (1-v)[m(1-v)+4]\frac{\rho^{m-3}}{R^{m+1}}\cos[m(\theta-\phi)], \\ \quad R\geq\rho \\ V_v^E(s,x)=\sum_{m=1}^{\infty} m^2(m+1)(1-v)[m(1-v) \\ \quad -4]\frac{R^{m-1}}{\rho^{m+3}}\cos[m(\theta-\phi)]+\sum_{m=2}^{\infty} m^2(m-1) \\ \quad (1-v)[m(1-v)+4]\frac{R^{m-3}}{\rho^{m+1}}\cos[m(\theta-\phi)], \\ \quad \rho>R \end{cases}$$

It is noted that the properties of series expansion in terms of degenerate kernel should be taken care when ρ is equal to R. The discussions for $\rho = R$ are shown below:

(1) The kernels (U, Θ_θ, M_m, V_v) are symmetric since $\rho = R^+$ and $\rho = R^-$ result in the same expression of $\rho = R$.
(2) The U_θ, Θ and M kernels are continuous when x moves across the boundary. Therefore, the interior kernel is equal to the exterior one when R is equal to ρ.
(3) For the other kernels, they have free terms when x moves across the boundary. We can not say anything at $\rho = R$ since the potential is not continuous [16].

References

1. Beskos DE (1991) Boundary element analysis of plates and shells. Spring, Berlin Heidelberg New York
2. Christiansen S (1975) Integral equation without a unique solution can be made useful for solving some plane harmonic problems. J Inst Math Appl 16:143–159
3. Christiansen S (1998) Derivation and analytical investigation of three direct boundary integral equations for the fundamental biharmonic problem. J Comp Appl Math 91:231–247
4. Chudinovich I, Constanda C (1999) Non-stationary integral equations for elastic plates. C. R. Acad Sci 329:1115–1120
5. Chudinovich I, Constanda C (2000) Integral representations of the solutions for a bending plate on an elastic foundation. Acta Mech 139(1–4):33–42
6. Chudinovich I, Constanda C (2000) Existence and uniqueness of weak solutions for a thin plate with elastic boundary conditions. Appl Math Lett 13:43–49
7. Chudinovich I, Constanda C (2000) Solvability of initial boundary value problem in bending of plates. Z. Angew Math Phys 51:449–466
8. Chudinovich I, Constanda C (2001) The solvability of boundary integral equations for the Dirichlet and Nuemann problems in the theory of thin elastic plates. Math Mech Solids 6(3):269–279
9. Chen JT, Lin JH, Kuo SR, Chiu YP (2001) Analytical study and numerical experiments for degenerate scale problems in boundary element method using degenerate kernels and circulants. Eng Ana Bound Elem 25(9):819–828
10. Chen JT, Lin JH, Kuo SR, Chyuan SW (2001) Boundary element analysis for the Helmholtz eigenvalue problems with a multiply-connected domain. Proc R Soc Lond A 457:2521–2546
11. Chen JT, Lee CF, Chen IL, Lin JH (2002) An alternative method for degenerate scale problem in boundary element methods for the two-dimensional Laplace equation. Eng Ana Bound Elem 26(7):559–569
12. Chen JT, Kuo SR, Lin JH (2002) Analytical study and numerical experiments for degenerate scale problems in the boundary element method for two-dimensional elasticity. Int J Numer Meth Eng 54(12):1669–1681
13. Chen JT, Lin SR, Chen KH (2005) Degenerate scale problem when solving Laplace's equation by BEM and its treatment. Int J Numer Meth Eng 62(2):233–261
14. Chen JT, Chen KH, Chen IL, Liu LW (2003) A new concept of modal participation factor for numerical instability in the dual BEM for exterior acoustics, Mech Res Comm 30(6):161–174
15. Chen JT, Wu CS and Lee YT (2005) The equivalence of the Trefftz method and method of fundamental solutions for Laplace and biharminic equations. Comput Math Appl, Accepted
16. Chen JT, Wu CS and Chen KH (2005) A study of free terms for plate problems in the dual boundary integral equations, Eng Ana Bound Elem, 29:435–446
17. Constanda C (1994) On non-unique solutions of weakly singular integral equations in plane elasticity. Q J Mech Appl Math 42:261–268
18. Constanda C (1997) On the Dirichlet problem for the two-dimensional biharmonic equation. Math Meth Appl Sci 20:885–890
19. Costabel M, Dauge M (1996) Invertibility of the biharmonic single layer potential operator Integr Equat Oper Th 24:46–67
20. Golberg MA (1978) Solution methods for integral equations: theory and applications. New York: Plenum Press
21. He WJ, Ding HJ, Hu HC (1996) Non-uniqueness of the conventional boundary integral formulation and its elimination for plane elasticity problems. Comput Struc 59(6):1059–1062
22. He WJ, Ding HJ, Hu HC (1996) A necessary and sufficient boundary integral formulation for plane elasticity problems. Comm Num Meth Eng 12:413–424
23. He WJ, Ding HJ, Hu HC (1996) Degenerate scales and boundary element analysis of two dimensional potential and elasticity problems. Comput Struc 60(1):155–158
24. He WJ (2000) An equivalent boundary integral formulation for bending problems of thin plates. Comput Struc 74:319–322
25. Jaswon MA, Symm GT (1977) Integral equation methods in potential theory and elastostatics. Academic press, Lodon
26. Mitra AK, Das S (1988) Nonuniqueness in the integral equations formulation of the biharmonic equation in multiply connected domains. Comput Meth Appl Mech Eng 69:205–214
27. Mukherjee S, Mukherjee YX (1998) The hypersingular boundary contour method for three-dimensional linear elasticity. J Appl Mech ASME 65:300–309
28. Mills RD (1977) Computing internal viscous flow problems for the circle by integral methods. J Fluid Mech 12:609–624
29. Phan A-V, Mukherjee S, Mayer JRR (1998) The hypersingular boundary contour method for two-dimensional linear elasticity. Acta Mech 130:209–225
30. Tomlinson K, Bradley C, Pullan A (1996) On the choice of a derivative boundary element formulation using Hermite interpolation. Int J Numer Meth Eng 19(3):451–468
31. Vodička R, Mantič V (2004) On Invertibility of elastic single-layer potential operator. J Elasticity 74:147–173
32. Wu CS (2004) Degenerate scale analysis for membrane and plate problems using the meshless method and boundary element method, Master Thesis, Department of Harbor and River Engineering, National Taiwan Ocean University, Keelung, R.O.C